Dual-loop Control for Backlash Correction in Trajectory-tracking of a Planar 3-RRR Manipulator

Abhishek Agarwal, Chaman Nasa, Sandipan Bandyopadhyay

Abstract

The presence of backlash in the gearheads is an inherent problem in manipulators using geared motors. This paper looks at a potential solution to this problem via the implementation of a *dual-loop* control strategy, in which feedback is taken from the motors as well as the end-effector of the manipulator. Using the redundant sensed information, the *actual* error in the joint-space is computed and used to rectify the desired trajectory for the joint-space trajectory-tracking control scheme. Experiments done on a 3-RRR planar parallel manipulator show significant improvement in the tracking performance due to the introduction of dual-loop control scheme.

Keywords: Dual-loop, trajectory tracking, backlash correction, parallel manipulators

1 Introduction

In many typical robotic applications, geared servo motors are used as the actuators. The gearhead is essential to reduce the speed of the motor to the desired speed of the actuated links and generate the required torque. However, an inherent problem in a gearhead is the friction and the backlash. Due to the backlash, the actuated link positions are not accurately known, even when the corresponding motor position is sensed accurately by the motor encoder. Therefore, a position control scheme for the motor cannot ensure accurate positioning of the end-effector. The actual state of the end-effector is required for improving the accuracy, and this requires the end-effector feedback to be available in the control scheme. Towards this purpose a control scheme known as *dual-loop* control has been developed by several researchers [1, 2] and industry experts [3].

Dual-loop control is a cascaded control scheme consisting of *two* position control loops. The *inner* motor position loop is a high-bandwidth loop [4], which along

Abhishek Agarwal*
Systemantics India Pvt. Ltd, Bangalore, India,
E-mail: abhishek@systemantics.com.

Chaman Nasa*
Eaton Technologies Private Limited, Pune, India,
E-mail: chamannasa@eaton.com.

Sandipan Bandyopadhyay
Department of Engineering Design, Indian Institute of Technology Madras India,
E-mail: sandipan@iitm.ac.in.

*The work presented in this paper was done by the authors during their working period at Indian Institute of Technology Madras, India.

with the *outer* load position loop, can effectively compensate for backlash. The *outer-loop* takes feedback directly from the task-space, and brings it into the joint space via inverse kinematics. In doing so, it captures the position errors introduced by backlash, among other possible sources of disturbance. An attempt to reduce this error in the outer-loop results in an update of the reference trajectory for the inner loop, and improves the overall positioning/tracking performance.

We use a distributed linear position control scheme, where the PID configuration is divided between the inner and the outer loop. The integral control is confined to the outer loop, while the inner loop is under the standard PD control. This scheme, known as the *improved dual-loop* control [3], is implemented on a planar parallel manipulator, namely a 3-RRR. The manipulator is made to track a non-singular circular path with and without the integral control, (i.e., the outer loop). It is seen that the tracking performance is much better under the dual-loop control than otherwise.

The paper is structured as follows: in Section 2, the kinematic model of the manipulator and the mathematical formulations are discussed. In Section 3, the experimental setup is described and the experimental results are described. The conclusions are presented in Section 5.

2 Mathematical Formulation

The kinematic model of the manipulator is shown in Fig. (1(b)). The fixed base, $\boldsymbol{b_1 b_2 b_3}$, and moving platform, $\boldsymbol{p_1 p_2 p_3}$, are equilateral triangles and the three fingers are identical. b, l, r, and, a are lengths of the sides of the base triangle, active links, passive links, and the sides of the moving platform, respectively. The geometry of the manipulator is identical to those reported in [5] and [6]. The actuator coordinates, $\boldsymbol{\theta}$

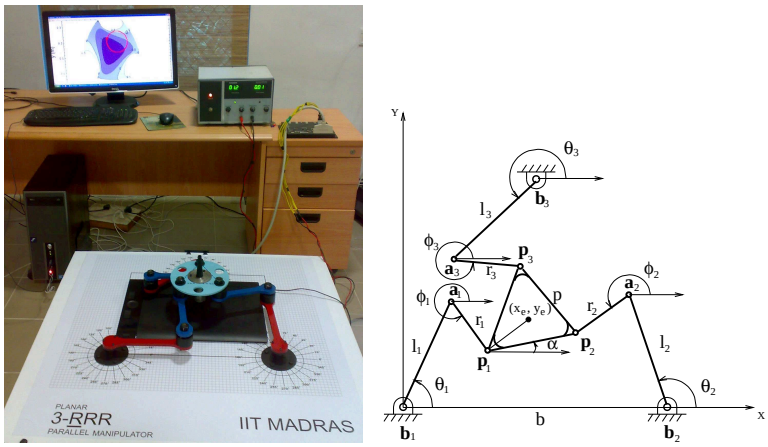

(a) Experimental setup of the 3-RRR manipulator

(b) Schematic representation of the 3-RRR manipulator

Figure 1: Experimental setup and schematic of 3-RRR planar parallel manipulator

$= (\theta_1, \theta_2, \theta_3)^T$, and the task space coordinates of the end-effector, $\boldsymbol{x} = (x, y, \alpha)^T$, are related by the loop closure constraints, $\boldsymbol{\eta}(\boldsymbol{\theta}, \boldsymbol{x}) = \mathbf{0}$, given by:

$$(\boldsymbol{a_i} - \boldsymbol{p_i})^{\boldsymbol{T}}(\boldsymbol{a_i} - \boldsymbol{p_i}) - r_i^2 = 0, \text{ where, } i = 1, 2, 3 \tag{1}$$

which are of the form:

$$a_i \cos\theta_i + b_i \sin\theta_i + c_i = 0, \text{ where, } i = 1, 2, 3 \tag{2}$$

where, a_i, b_i, and c_i, are closed-form expressions of the architecture parameters (b, l, r, a) and $\boldsymbol{x}$. Eq. (2) gives two solutions for θ_i for each branch, which gives rise to $eight$ $(2 \times 2 \times 2)$ possible configurations for a given $\boldsymbol{x}$.

2.1 Velocity kinematics of the model

The differential kinematic relation of the manipulator takes the form:

$$\begin{aligned} &\frac{\partial \boldsymbol{\eta}}{\partial \boldsymbol{\theta}}\dot{\boldsymbol{\theta}} + \frac{\partial \boldsymbol{\eta}}{\partial \boldsymbol{x}}\dot{\boldsymbol{x}} = \boldsymbol{J_{\eta\theta}}\dot{\boldsymbol{\theta}} + \boldsymbol{J_{\eta x}}\dot{\boldsymbol{x}} = \mathbf{0}, \text{ where,} \\ &\boldsymbol{J_{\eta\theta}} = \frac{\partial \boldsymbol{\eta}}{\partial \boldsymbol{\theta}}, \boldsymbol{J_{\eta x}} = \frac{\partial \boldsymbol{\eta}}{\partial \boldsymbol{x}} \end{aligned} \tag{3}$$

From Eq. (3), the rates of actuator and task space coordinates are related by:

$$\dot{\boldsymbol{x}} = -\boldsymbol{J}_{\boldsymbol{\eta x}}^{-1}\boldsymbol{J_{\eta\theta}}\dot{\boldsymbol{\theta}} = \boldsymbol{J_{x\theta}}\dot{\boldsymbol{\theta}}, \ \det(\boldsymbol{J_{\eta x}}) \neq 0 \tag{4}$$

$$\dot{\boldsymbol{\theta}} = -\boldsymbol{J}_{\boldsymbol{\eta\theta}}^{-1}\boldsymbol{J_{\eta x}}\dot{\boldsymbol{x}} = \boldsymbol{J_{\theta x}}\dot{\boldsymbol{x}}, \ \det(\boldsymbol{J_{\eta\theta}}) \neq 0 \tag{5}$$

where, $\boldsymbol{J_{x\theta}} = -\boldsymbol{J}_{\boldsymbol{\eta x}}^{-1}\boldsymbol{J_{\eta\theta}}$ and $\boldsymbol{J_{\theta x}} = -\boldsymbol{J}_{\boldsymbol{\eta\theta}}^{-1}\boldsymbol{J_{\eta x}}$.

2.2 Singularity-free trajectory planning

In this paper, a singularity-free path has been chosen to demonstrate the dual-loop control scheme. A non-singular circular path is chosen by superposing it on the contour of the singularity function, as shown in [5] and [6]. As seen in Fig. (2), the circular path does not intersect the zero-valued contour line. Hence, it is not singular for the chosen orientation, $\alpha = 0$. The chosen trajectory is cubic in time, such that the manipulator starts from and stops at rest.

3 Experimental Setup

Fig. (1(a)) shows a physical prototype of the 3-RRR manipulator used in the control experiments.

3.1 Details of the hardware

The manipulator has the following architecture parameters: $b = 0.50$ m, $l = 0.22$ m, $r = 0.17$ m, $a = 0.125$ m. The actuators are `Maxon` D.C. geared servo motors

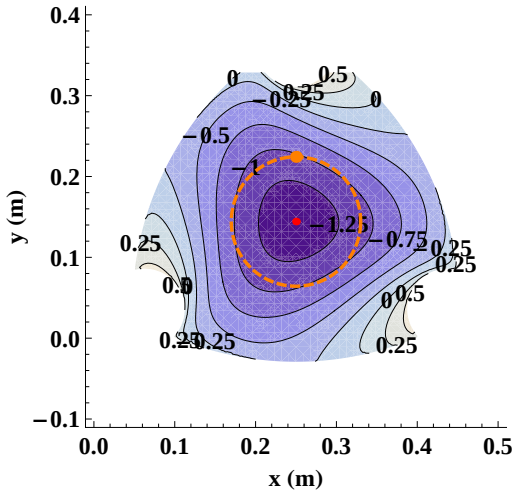

Figure 2: Contour of the singularity function for $\alpha = 0$

controlled by `Galil` DMC-1846 controller. The coordinates (x, y) are sensed through a digitiser tablet. There is no sensor for obtaining α directly, and as such, a trajectory with $\alpha(t) = 0$ is chosen. Though, $\alpha(t)$ can be computed by forward kinematics from the position feedback of the motors, it is computationally expensive as well as error-prone due to the backlash in the gearheads. The hardware details of the prototype have been listed at [7].

3.2 Dual-loop control scheme

The rotary encoders mounted on the motor shaft sense the motor position accurately. However, due to the backlash in the gearheads, the position of the corresponding links are in error. This makes the control problem difficult and deteriorates the tracking performance.

The dual-loop control scheme [3] suggests that sensors are placed at both the motors and the end-effector, thus allowing the control loop to act upon the motor position and end-effector position simultaneously. For the experimental setup used in this paper, a feedback control system as represented in Fig. (3) is used. A PID control scheme is chosen which is divided between the task space feedback (outer) loop and the motor feedback (inner) loop. The PD control gains for the inner loop are chosen so that the error dynamics is overdamped. However, errors due to backlash are not seen in the inner loop and thus are not corrected. The task space feedback gives an estimate of position error due to backlash as well as the steady state error. An integral control action on this error attempts to nullify this error without introducing oscillations.

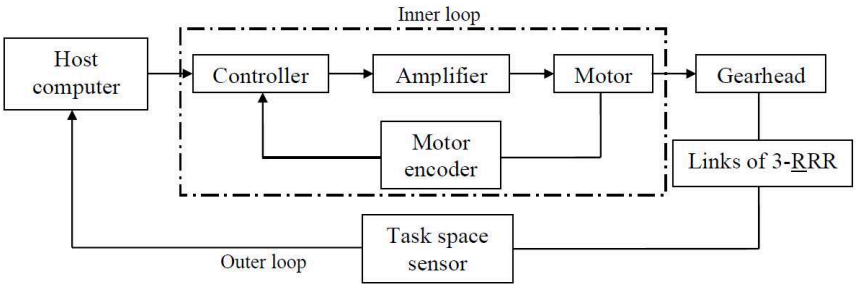

Figure 3: Schematic representation of dual-loop control scheme

3.3 Implementation of the dual-loop control scheme

The integral control acts on the task space feedback. The digitiser tablet senses the task space coordinates $(x(t), y(t))$. As $\alpha(t)$ is held fixed at zero (i.e., by assumption), $\boldsymbol{x}(t) = (x(t), y(t), \alpha(t))^T$ is known at each time step. The actual state of the motors can be obtained by inverse kinematics, as shown in Section (2). The zeroth order inverse kinematics, essentially, gives the effect of backlash at the end-effector arising from all the three motors. The integral control is then implemented as:

$$\begin{aligned} \boldsymbol{\theta}_r(t) &= \boldsymbol{\theta}_d(t) + \boldsymbol{K}_i \int_0^t \boldsymbol{e}_a(\tau)\, d\tau, \text{ where,} \\ \boldsymbol{e}_a(t) &= \boldsymbol{\theta}_d(t) - \boldsymbol{\theta}_c(t) \end{aligned} \tag{6}$$

Eq. (6) is the integral control action on the task space feedback, where, $\boldsymbol{\theta}_r(t)$ is the rectified position which the motors have to achieve, $\boldsymbol{\theta}_d(t)$ is the desired position of the motors for desired x and y, $\boldsymbol{\theta}_c(t)$ is the calculated position of the motors from inverse kinematics, and, $\boldsymbol{e}_a(t)$ is the actual error. Eq. (6) is integrated by the Euler formula as the time step is very small.

The controller in the inner loop uses a typical PD control scheme [8] to achieve the desired position, which is given by:

$$\begin{aligned} \boldsymbol{V}(t) &= \boldsymbol{K}_p \boldsymbol{e}_m(t) + \boldsymbol{K}_d \dot{\boldsymbol{e}}_m(t), \text{ where,} \\ \boldsymbol{e}_m(t) &= \boldsymbol{\theta}_r(t) - \boldsymbol{\theta}_s(t) \end{aligned} \tag{7}$$

$\boldsymbol{V}(t)$ is the output signal from the controller, $\boldsymbol{\theta}_s(t)$ is the position feedback from rotary encoders, $\boldsymbol{e}_m(t)$ is the position error of the motor in the inner loop, and, $\dot{\boldsymbol{e}}_m(t)$ is the corresponding velocity error.

4 Experimental Results and Discussion

The paths chosen are circles with their center at the centroid of the base triangle $\boldsymbol{b_1 b_2 b_3}$ and radius 0.08 m and 0.04 m. Fig. (5) and (6) show an improvement in

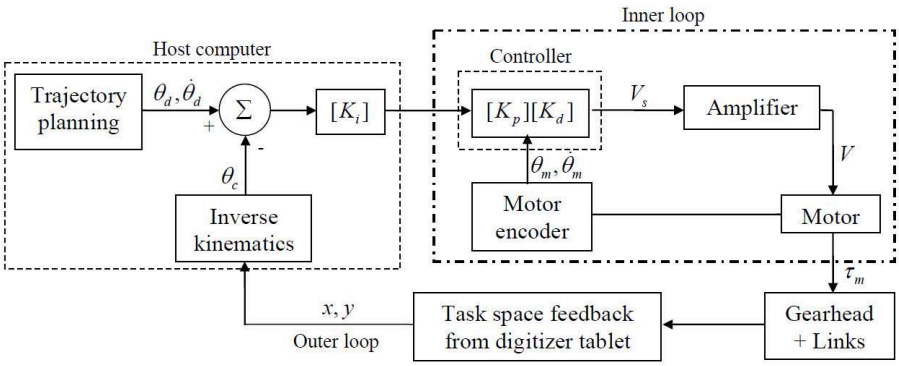

Figure 4: Improved dual-loop representing PID control distribution

trajectory tracking performance when dual-loop is applied. Note that the two trajectory tracking experiments for the circles were conducted separately, and the results superposed for comparative study. Each experiment was run ten times. The results, as in Table 1, are averaged over ten runs each.

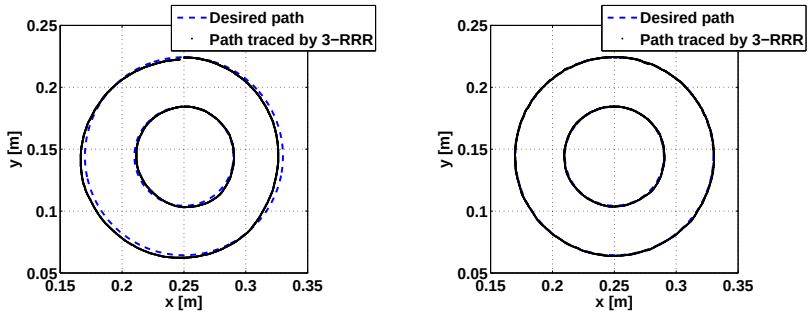

(a) Without backlash correction ($K_i = 0.0$) (b) With backlash correction ($K_i = 4.0$)

Figure 5: Desired path vs. path traced; Average linear velocity$= 0.021$ m/s; $K_p = 6.0$, $K_d = 64.00$

From Table 1, it is a clear observation that at a lower velocity the tracking error reduces as the disturbance due to inertial effects is not seen due to large reduction ratio of the motors [9]. For circle of radius 0.08 m, at average linear velocity, $v = 0.021$ m/s, 92.1% improvement in the average RMS error is seen, while at $v = 0.042$ m/s, 90.4% improvement in average RMS error is obtained due to backlash correction.

An interesting observation is that on reducing the radius of the desired circular path to 0.04 m from 0.08 m, while keeping the velocity same, dual-loop control yields nearly the same average RMS and maximum errors.

Fig. (7) gives a comparison of the trajectory of each motor for circular trajectory of

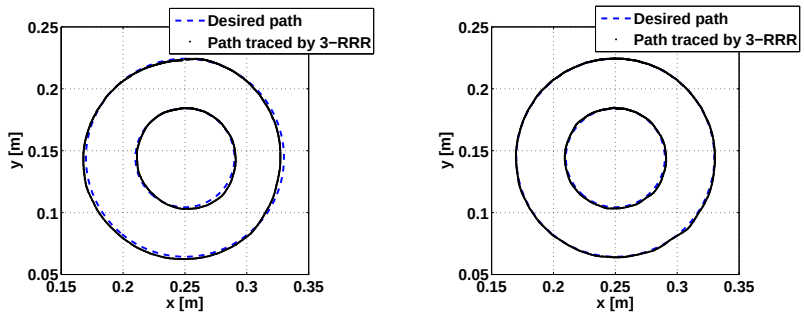

(a) Without backlash correction ($K_i = 0.0$) (b) With backlash correction ($K_i = 4.0$)

Figure 6: Desired path vs. path traced; Average linear velocity$= 0.042$ m/s; $K_p = 6.0$, $K_d = 64.00$

Table 1: Comparison of results from experiments

Fig.	*Backlash correction*	*Radius (m)*	*Velocity m/s*	*RMS error (mm) (averaged)*	*Max. error (mm) (averaged)*
5(a)	No	0.08	0.021	4.71	8.69
5(b)	Yes	0.08	0.021	0.37	1.22
5(a)	No	0.04	0.021	2.57	4.80
5(b)	Yes	0.04	0.021	0.45	1.21
6(a)	No	0.08	0.042	4.72	8.87
6(b)	Yes	0.08	0.042	0.58	2.11
6(a)	No	0.04	0.042	3.47	6.32
6(b)	Yes	0.04	0.042	1.02	2.09

radius 0.08 m and average linear velocity 0.021 m/s. $\boldsymbol{\theta}_c(t)$, calculated by inverse kinematics from the end-effector feedback, and, $\boldsymbol{\theta}_s(t)$, sensed from the rotary encoders of the motors, are plotted against $\boldsymbol{\theta}_d(t)$, the desired position of the motors. It is observed that $\boldsymbol{\theta}_c(t)$ follows the desired trajectory, implying that the integral control acting on the task space feedback tries to nullify the errors not seen by the PD inner loop. Consequently, from the plot of $\boldsymbol{\theta}_s(t)$, it is evident that the rectified motor position from integral control, $\boldsymbol{\theta}_r(t)$, is adjusted in order to correct the effect of backlash.

5 Conclusions

A dual-loop control strategy, aimed at reducing tracking errors due to backlash in the geared actuators has been presented. Experimental studies show that the PID control, with the integral controller in the outer-loop and the PD controller in the inner improves the tracking performance significantly. As expected, the improvement is more significant at lower manipulator speeds than higher, as at higher speeds, inertial forces

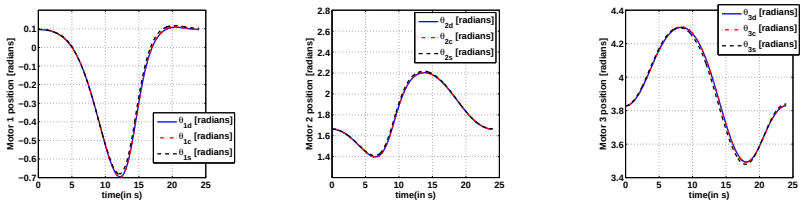

(a) Motor 1 trajectory (b) Motor 2 trajectory (c) Motor 3 trajectory

Figure 7: Comparison of desired, calculated, and sensed trajectory of motors $1, 2, 3$

(unaccounted for in the linear control scheme) cause greater disturbances.

The methodology presented here can potentially be applied to any manipulator with a geared actuator. The use of this scheme in conjunction with a dynamic model of the manipulator would be the next research objective.

References

[1] R. Desantis, "Dual loop PID configuration," in *United States Patent. Patent number: 5481453*, January 1996.

[2] R. Boneh and O. Yaniv, "Control of an elastic two-mass system with large backlash," *Journal of Dynamic Systems, Measurement and Control*, vol. 121, no. 2, pp. 278–284, 1999.

[3] J. Tal, "Two feedback loops are better than one," in *Machine Design, http://www.galilmc.com/learning/articles/md040899.pdf*, April 1999.

[4] M. Nordin and P.-O. Gutman, "Controlling mechanical systems with backlash–a survey," *Automatica*, vol. 38, no. 10, pp. 1633 – 1649, 2002.

[5] C. Nasa, "Trajectory-tracking control of a planar 3-RRR parallel manipulator with singularity avoidance," M. S. thesis, Indian Institute of Technology, Madras, Chennai, India, April 2011.

[6] C. Nasa and S. Bandyopadhyay, "Trajectory-tracking control of a planar 3-RRR parallel manipulator with singularity avoidance," in *13th World Congress in Mechanism and Machine Science*, June 2011.

[7] "http://www.ed.iitm.ac.in/˜sandipan/research/3rrr.html."

[8] A. Ghosal, *Robotics: Fundamental Concepts and Analysis*. New Delhi: Oxford University Press, 2006.

[9] Y. Nakamura, H. Hanafusa, and T. Yoshikawa, "Task-priority based redundancy control of robot manipulators," *International Journal of Robotics Research*, vol. 6, no. 2, pp. 3–15, 1987.